Atmospheric Environment 116 (2015) 293–307

Contents lists available at ScienceDirect

Atmospheric Environment

journal homepage: www.elsevier.com/locate/atmosenv

Understanding interannual variations of biomass burning from Peninsular Southeast Asia, part I: Model evaluation and analysis of systematic bias

Xinyi Dong, Joshua S. Fu*

Department of Civil and Environmental Engineering, The University of Tennessee, Knoxville, TN, 37996, USA

HIGHLIGHTS

- Multi-years biomass burning over PSEA is examined with a synthetic study using various datasets.
- Systematic biases are identified within the spatial allocation of INTEX-B emission.
- Biomass burning NOx emission factor is overestimated and cause CMAQ overpredict NO_2.
- CMAQ dust module underestimated dust emission and PM_{10} by 50%–60% over north China.

ARTICLE INFO

Article history:
Received 5 January 2015
Received in revised form
19 May 2015
Accepted 16 June 2015
Available online 20 June 2015

Keywords:
Peninsular Southeast Asia
Biomass burning
WRF/CMAQ
Interannual variation

ABSTRACT

The Weather Research and Forecasting model and the Community Multiscale Air Quality model (WRF/CMAQ) modeling system was applied over Peninsular Southeast Asia (PSEA) and East Asia (EA) for 5 consecutive years from 2006 to 2010 in March and April to understand the PSEA biomass burning for its interannual variations, transport pathway, and impacts at local and downwind areas. As many of the modeling applications over PSEA or EA were usually evaluated with limited regional or local observations focusing on short simulation periods, in this work we incorporated ground surface measurements from multiple networks covering different sub-regions and satellite retrievals to comprehensively examine the performance of WRF/CMAQ and probe into the possible uncertainties of the modeling system. We found increasing simulation discrepancy for CO, NO_2, and SO_2 from 2006 to 2010 at south part of PSEA ($\leq$17°N) due to outmoded anthropogenic emission in INTEX-B, while local surface observations and CO_2 emission data from World Bank suggested substantial growth of anthropogenic emission over PSEA during the 5 years. The spatial allocation of emission based on population distribution was also found to introduce large uncertainty with overestimation at populated urban area and underestimation at industry area. Over north PSEA (>17°N) CMAQ systematically overestimated CO, surface NO_2, tropospheric column NO_2 by around 6%–20%, 8–15%, and 40%–50% respectively, indicating positive bias within the biomass burning emission due to overestimated emission factor as suggested by OMI retrievals. At EA, despite moderate overestimations for surface NO_2 and SO_2 by 20%–30% and moderate underestimation for AOD by 30%–50%, no significant temporal trend was found. We found CMAQ underestimated PM_{10} concentrations at north and northeast EA by 50%–60% due to impact of dust storm, yet the dust plume rise scheme within the model was unable to reproduce it. Our results suggested that an urgent research effort is needed for updating the anthropogenic emission of PSEA countries, and the dust emission module within CMAQ need further improvement for applications over EA.

1. Introduction

Biomass burning over Southeast Asia (SEA) has significant impacts on atmospheric visibility, public health, aquatic system, and also regional climate over the local and downwind areas in East Asia (EA). At Peninsular Southeast Asia (PSEA: Cambodia, Laos,

* Corresponding author.
E-mail address: jsfu@utk.edu (J.S. Fu).

http://dx.doi.org/10.1016/j.atmosenv.2015.06.026
1352-2310/

Myanmar, Thailand, Vietnam, also referred as Indochina in some literatures), biomass burning usually peak in March and April with a sharply decrease in May due to the onset of summer monsoon, introducing about two-thirds of the total organic carbon (OC) and 50% of the element carbon (EC) over the local area (Gustafsson et al., 2009). Precursors emissions including nitrogen oxides (NO_x) and sulfur dioxide (SO_2) from biomass burning may also lead to intensive aerosol and ozone (O_3) formation. While many of the local countries are highly populated, the downwind region including Pearl River Delta, Yangtze River Delta, Hong Kong, and Taiwan are also metropolitan areas with millions of residents. PSEA biomass burning could be transported to EA through subtropical westerlies and Asian monsoon, and some studies have demonstrated it played an important role in affecting air quality in downwind areas (Deng et al., 2008; Fu et al., 2012a; Huang et al., 2014; Streets et al., 2003; Tang et al., 2003a; Wang et al., 2007; Zhang et al., 2013). PSEA biomass burning has very broad influences in terms of both spatial and population coverage, and these influences need to be carefully evaluated to help understand the deleterious impacts on human health and the interactions between biomass burning and regional climate in tropical and subtropical areas.

In recent years a few studies have been conducted with modeling or observational methods to investigate the impact of biomass burning over PSEA and EA, which mainly focused on evaluating its overall contribution of air pollutants to local and downwind areas. Fu et al. (2012a) investigated the 2006 PSEA biomass burning impacts with modeling method and reported long-range transport could contribute to 64 $\mu g/m^3$ of particulate matter with aerodynamic diameter less than or equal to 2.5 μm ($PM_{2.5}$) over Eastern China; Huang et al. (2013) examined the same episode with models and ground measurements, reporting that the contribution from biomass burning on AOD was about 56% for local area, and 26%–62% for the downwind area; Tang et al. (2003b) used TRACE-P flight measurements and regional model to evaluate the 2001 biomass burning episode, and reported the averaged net influence in March was 50% for OH, 40% for HO_2, 60% for HCHO, and 10 ppbv for O_3; Hsu et al. (2003) used satellite data to evaluate the impacts of biomass burning on radiative forcing in March 2000, and reported that the reflected solar radiation from clouds due to smoke aerosols can be reduced (enhanced) by up to 100 (20) W/m^2. Chuang et al. (2013) analyzed the chemical characteristics of biomass burning aerosols measurements taken in March and April 2010 over Indochina and reported that the potassium ion (K^+) and water-soluble organic carbon (WSOC) from biomass burning was higher than other published studies, while the ratio of EC was similar to other literatures. During the past 10 years, some national or international collaborated field campaigns have also been conducted over PSEA trying to characterize the physical, chemical, and optical properties of biomass burning pollutants, which include the NASA TRACE-P (Jacob et al., 2003), UNEP ABC (Nakajima et al., 2007), NASA BASE-ASIA (Li et al., 2013; Tsay et al., 2013; Sayer et al., 2012), and 7-SEAS (Lin et al., 2013; Reid et al., 2013).

These research efforts have built up the fundamental knowledge about PSEA biomass burning in terms of many different aspects such as emission, transport, visibility, impact on air quality, and hydrological cycle. However, most of the studies primarily focused on a specific short episode and very few of them have probed into the interannual variations or long-term changes of biomass burning at PSEA, and this limitation leaves two poorly understood issues: First, neither observational or modeling studies have described the possible annual changes or upper and lower limits of PSEA biomass burning, yet it is essential to have these information to fully understand the overall impact of biomass burning not only for the extreme episodes, but also on average scale for multiple years in order to access its long term impacts on air quality and regional climate. Second, although we often rely on model simulations for impact analysis, the uncertainties within the modeling system and the stability of model predictions under different conditions (e.g. emissions, meteorology) remain unknown, as most of the modeling studies focused on short episodes (from a few days to a few weeks) and model evaluation were performed with limited local observations. These two issues are of special importance because the PSEA biomass burning has substantial annual changes (Tsay et al., 2013), thus we may expect significant variations of its impacts and need to know how well model can reproduce these changes from year to year. According to World Health Organization (WHO), many Asian countries are experiencing severe air pollution problems and rapid changes of anthropogenic emissions (WHO, 2011; WHO, 2014), so understanding the interannual variations of PSEA biomass burning is also helpful to evaluate its relative importance and can provide viable suggestions for mitigation.

In this study, the 3-D modeling system Weather Research and Forecasting model and Community Multiscale Air Quality model (WRF/CMAQ) (Skamarock et al., 2008; Byun and Schere, 2006) was applied over PSEA and EA for 5 consecutive years from 2006 to 2010 in March and April to investigate the annual variations of biomass burning over the local and downwind area. Although some modeling studies have been conducted over this region, the WRF/CMAQ modeling system hasn't been thoroughly evaluated with domain-wide observations due to limited local measurements. Evaluation for multiple-year simulations is necessary to reveal the stability of model performance under different meteorology and emission conditions to identify the possible systematic errors and model sensitivities. So in Part I of this work, ground surface observations including measurements from Pollution Control Department of Ministry Natural Resources and Environment of Thailand (PCD; http://www.pcd.go.th/indexEng.cfm), Hong Kong Environmental Protection Department (HKEPD, Kwok et al., 2010), Acid Deposition Monitoring Network in East Asia (EANET, 2007), API (Air Pollution Index; http://datacenter.mep.gov.cn) from China Ministry of Environmental Protection (MEP), Taiwan Air Quality Monitoring Network (TAQMN; http://taqm.epa.gov.tw/taqm/en/default.aspx) organized by Taiwan EPA, and AErosol RObotic NETwork (AERONET; Holben et al., 2001) operated by NASA are collected to perform evaluation for CMAQ predictions. These networks are managed by different agencies and cover the majority of PSEA and EA over different sub-regions, thus enable a thorough model evaluation with wide spatial and temporal coverage. Satellite products including NO_x from Ozone Monitoring Instrument (OMI; http://disc.sci.gsfc.nasa.gov/Aura/data-holdings/OMI) and Aerosol Optical Depth (AOD) from Moderate Resolution Imaging Spectroradiometer (MODIS; http://modis.gsfc.nasa.gov/) are also employed for model evaluation in terms of column densities. The objective of this paper is to evaluate the model performance with various network observations over different regions to examine the model's capacity for multiple-year simulations, and also probe into the possible uncertainties within the modeling system. The analysis of PSEA biomass burning impact on local and regional air quality and its annual variations are provided in Part II.

2. Methodology

2.1. Emission inventories

As most of the PSEA and EA countries have no official release of public available anthropogenic emission inventories on local scale, many of the modeling efforts have to rely on the inventories developed by research studies, and sometimes even have to use global inventories for regional simulation. For regional scale

simulation in this area, some studies (Carmichael et al., 2008; Fu et al., 2008; Lamsal et al., 2010; Lu et al., 2011; Wang et al., 2010) used the TRACE-P emission dataset in Asia for year 2000 which was developed by NASA and the ACE-Asia project (Streets et al., 2003); other studies (Fu et al., 2012b; Huang et al., 2013; Wang et al., 2010) also used the Intercontinental Chemical Transport Experiment-Phase B (INTEX-B) emission for year 2006 which was also developed by NASA (Zhang et al., 2009); Ohara et al. (2007) developed an emission inventory from fuel combustion and industrial sources for Asia for the period 1980–2003. It is important to notice that despite many validation efforts attempting to improve their accuracies, these inventories are usually developed based on annual scale at coarse grid-cell for general precursors emissions with a top-down method, while regional modeling usually require a much finer resolution for both temporal/spatial allocation and chemical speciation. Also, since Asia countries have experienced rapid economic changes during the past decade, their anthropogenic emissions are also expected to change accordingly, but the research efforts for estimating emission changes are relatively limited and lag behind. Consequently, although these inventories provided important basis for understanding the anthropogenic emissions over PSEA and EA, their uncertainties may introduce significant discrepancies for model simulations. In this work, we use INTEX-B for anthropogenic emission except over China to investigate its possible uncertainties, and we use the inventory from Zhao et al. (2013a) over China because it is promptly updated.

Biogenic emission is generated by the Model of Emissions of Gases and Aerosols from Nature (MEGANv2.10) (http://bai.acd.ucar.edu/Megan/index.shtml). MEGAN has been applied in many different modeling studies over PSEA and EA and demonstrated its good estimation of natural emission source (Guenther et al., 2006; Muller et al., 2008).

Biomass burning emission is developed from the Fire Locating and Modeling of Burning Emissions (FLAMBE) project (Reid et al., 2009). While the Global Fire Emissions Database (GFED) is another popular biomass burning emission data source (van der Werf et al., 2008; van der Werf et al., 2010), Fu et al. (2012b) found out that GFED underestimated emission over PSEA and the simulation driven by FLAMBE inventory is found to have better agreement with surface observations. The finding is also consistent with the conclusion from Nam et al. (2010) who reported that biomass burning emission was substantially underestimated due to lack of agricultural fires based on a global simulation with GFED. In addition, FLAMBE contains hourly fire activities thus eliminate the uncertainties for temporal allocation.

2.2. Model description and evaluation protocol

WRFv3.4 and CMAQv5.0.1 were selected as modeling platform in this study. WRF/CMAQ system is configured with 36-km horizontal grid resolution and 34 vertical layers extending from ground surface to 50 mb with denser layers in lower atmosphere to better represent the mixing layer. The research domain covers PSEA and EA, as shown in Fig. 1. Initial and boundary condition was generated from GEOS-Chem global model following the routines described in Lam and Fu (2009).

For WRF evaluation, climate data from the National Climate Data Center (NCDC) is used to evaluate performance.

For CMAQ evaluation, the variables and observational networks employed are summarized in Table 1, with the locations of monitoring stations marked in Fig. 1 (different networks are represented by different markers: red cycles refer to API, navy blue triangles refer to PCD, green diamonds for EANET, dark blue rectangles for TAQMN, yellow rectangle for HKEPD, and purple triangles for AERONET; locations of observational stations from PCD, EANET, TAQMN, and HKEPD are listed in Table S1 in the supplementary material). These species and observational networks include: surface concentrations of CO, SO_2, NO_2, O_3, and particulate matter with aerodynamic diameter less than or equal to 10 μm (PM_{10}) from 25 sites of PCD in Thailand on a daily basis; PM_{10} derived from API at 86 cities and SO_2, and NO_2 concentrations derived from local data at 6 megacities (Beijing, Guangzhou, Shanghai, Guiyang, Wuhan, Xi'an) in China. These 6 cities reported API values for PM_{10}, SO_2, and NO_2 pollutants respectively (Wang et al., 2011). API is the only public available data in China with national coverage of majority cities and has been applied for model evaluation in several studies, despite some uncertainties (Dong et al., 2014; Zhao et al., 2013b); O_3, SO_2, NO_2, and PM_{10} from the EANET which contains 23 sites from multiple countries covering our research domain and simulation period; O_3, SO_2, NO_2, CO, $PM_{2.5}$, and PM_{10} from 2 super-sites (Sinjhuang and Ciaotou) of TAQMN in Taiwan. O_3, SO_2, NO_2, CO, and $PM_{2.5}$ from 4 sites (Tap Mun, Yuen Long, Tung Chung, and Tsuen Wan; observations at these 4 sites are averaged to represent Hong Kong because they were in same grid of CMAQ) of HKEPD in Hong Kong. Aerosol Optical Depth (AOD) was evaluated with both ground measurements from AERONET and satellite retrievals from MODIS. AERONET is an international global network measuring the aerosol optical properties using ground-based instrument, providing AOD measurements with the accuracy of ±0.03, and also measurements for Absorption AOD (AAOD) and Single Scattering Albedo (SSA). In this work, data from 70 AERONET sites were available for the simulation period. Daily average product from MODIS which contains AOD at 550 nm wavelength with $1^\circ \times 1^\circ$ resolution was utilized for CMAQ evaluation. CMAQ modeled AOD were derived following the approach described in Huang et al. (2013). Daily average product from OMI with $0.25^\circ \times 0.25^\circ$ resolution was used to evaluate vertical column density of tropospheric NO_2.

3. Model evaluation

As no significant bias or annual variations were found, evaluation for meteorology predictions from WRF was summarized in supplementary materials with Figure S1 and Table S2. In this section we discuss the evaluation of CMAQ of surface concentrations and volume densities.

3.1. Evaluation for surface concentrations

3.1.1. Annual changes of model performance

Surface observations from different networks enable the evaluation to examine model performance at different sub-regions within the modeling domain, and multi-year simulations help to probe into the systematic errors and self-consistency of the modeling system. Overlay of CMAQ simulations and observations were summarized in Fig. 2 for surface O_3 (1st column), NO_2 (2nd column), SO_2 (3rd column), CO (4th column), and PM_{10} (5th column) concentrations at monthly scale. According to Fig. 2, CMAQ generally reproduced the spatial distributions of all the pollutants. High values of these pollutants are found over north part of PSEA and industrial areas over EA, indicating the dominant impacts of biomass burning and anthropogenic emission at PSEA and EA respectively. Fig. 2 also demonstrated substantial annual variations of pollutants concentrations especially over PSEA and southwest China. To understand the model performance in different years over different areas, evaluation statistics including the averages of observation, simulation, correlation coefficient (R), and Normalized Mean Bias (NMB) were calculated for each year with raw data pairs on daily scale. According to spatial distributions shown in Fig. 2, biomass burning plumes covered the north part of PSEA and were transported eastward to southwest China, while the south part of

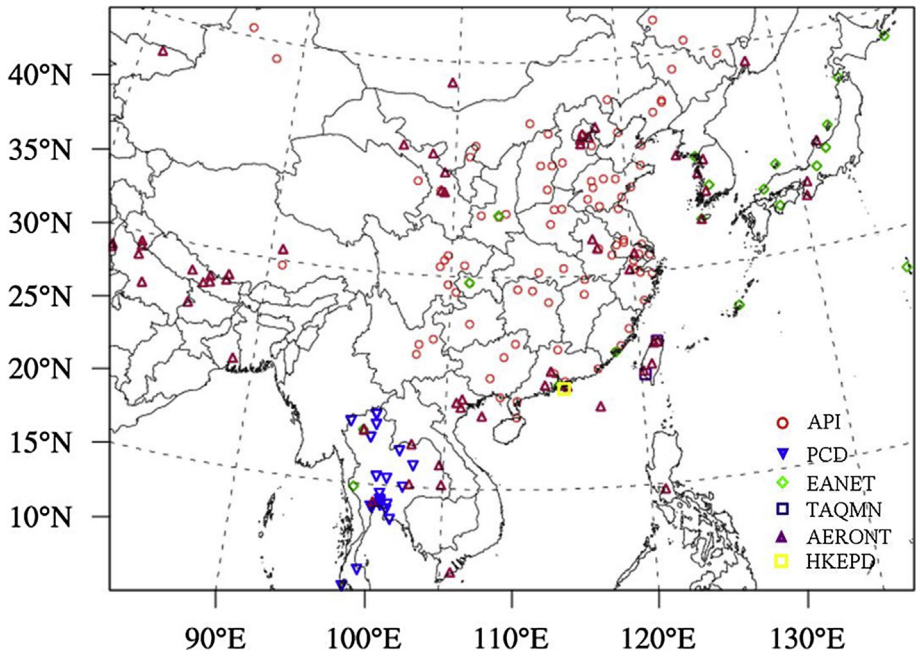

Fig. 1. Research domain and observation networks, different networks are represented by different markers: red cycles refer to API, navy blue triangles refer to PCD, green diamonds for EANET, dark blue rectangles for TAQMN, yellow rectangle for HKEPD, and purple triangles for AERONET. (For interpretation of the references to color in this figure legend, the reader is referred to the web version of this article.)

PSEA got very limited impact and anthropogenic emission played a more important role there. Thus we calculated the evaluation statistics for north (>17°N) and south (≤17°N) part of PSEA respectively to narrow down the uncertainties from biomass burning and anthropogenic emissions respectively, as summarized in Table 2.

Evaluation statistics shown in Table 2 suggested distinct model performance between two parts of PSEA in terms of interannual changes: model accuracy was more stable over north part of PSEA despite some fluctuations, but had obvious annual trend over south part of PSEA with better performance in 2006 and worse performance as the time approaching 2010. Over north PSEA, evaluation of CO showed NMB values around 20% for different years except 2007 when the NMB was 5.7%, indicating a systematic overestimation within the biomass burning CO emission. For other pollutants over north PSEA, model has moderate overestimations for SO_2, NO_2, and O_3 with NMB values of 26.2%–45.6%, 14.4%–17.8%, 17.8%–30% respectively, and moderate underestimation for PM_{10} with NMB values of −37%–20.9%, consistent with the overestimation of CO at north PSEA. Although there are some fluctuations of NMB values from year to year, no significant temporal trend was found for model's bias over north PSEA. Since biomass burning plays a dominant role at north PSEA, modeling discrepancy for these pollutants should largely attributed to overestimations within biomass burning emission. Over south PSEA however, NMB value for CO evaluation was only 0.73% for 2006 but underestimation occurred thereafter and was gradually getting larger from −11.3% in 2007 to −19.3% in 2010. The gradually increased NMB values indicated an elevated discrepancy within the model from 2006 to 2010, and evaluation for other pollutants also showed similar trend. Minor overestimations were found for SO_2 in 2006 and 2007 with NMB values less than 8%, but larger overpredictions were found increased from 31.1% in 2008 to 54.2% in 2010. Simulations for NO_2 had small NMB as −9.6% in 2006 and moderate underprediction with NMB of −38.4–29.3% for year 2007–2010. Similar trend was also found for O_3 prediction, which had moderate NMB value as 16.5% in 2006 and larger values of NMB

Table 1
Description of the observational datasets for CMAQ evaluation.

Dataset	Species measured	Observational frequency	Number of sites	Data source
API	PM_{10}, SO_2, NO_2	Daily	PM_{10}: 86 cities SO_2, NO_2: 6 cities	http://datacenter.mep.gov.cn
EANET	PM_{10}, SO_2, NO_2, O_3	Hourly/Daily/Monthly	Hourly: 11 sites in Japan Daily: 4 sites in China, 4 sites in Thailand, 1 site in Russia Monthly: 3 sites in South Korea	http://www.eanet.asia/
TAQMN	PM_{10}, SO_2, NO_2, CO, O_3, $PM_{2.5}$	Hourly	2 sites (Sinjhuang and Ciaotou)	http://taqm.epa.gov.tw/taqm/en/default.aspx
HKEPD	SO_2, CO, O_3, $PM_{2.5}$	Daily	4 sites (Tap Mun, Yuen Long, Tung Chung, Tsuen Wan)	http://epic.epd.gov.hk/EPICDI/air/station/?lang=en
PCD	PM_{10}, SO_2, NO_2, CO, O_3	Daily	25 sites	http://www.pcd.go.th/indexEng.cfm
AERONET	AOD	Daily	70 sites within our simulation domain	http://aeronet.gsfc.nasa.gov/cgi-bin/combined_data_access_new
MODIS	AOD	Daily	–	http://ladsweb.nascom.nasa.gov/data/search.html
OMI	Column NO_2	Daily	–	http://disc.sci.gsfc.nasa.gov/Aura/data-holdings/OMI/omno2_v003.shtml

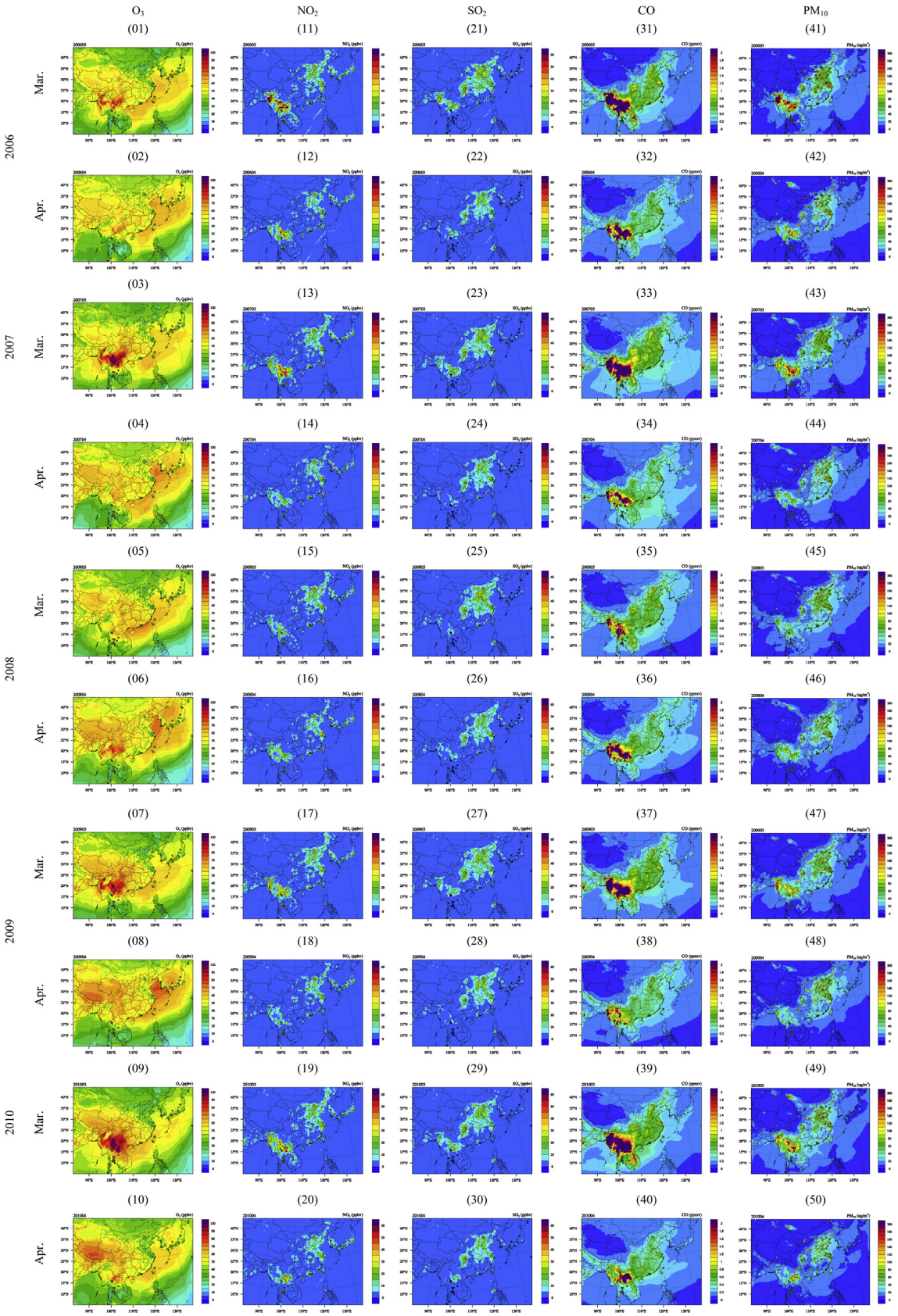

Fig. 2. Overlay of simulated and observed concentrations of O_3 (1st column), NO_2 (2nd column), SO_2 (3rd column), CO (4th column), and PM_{10} (5th column) at surface level in March and April from 2006 to 2010. Markers denote observations from different networks: cycles indicate measurements from API, diamonds represent EANET, rectangular boxes represent TAQMN and HKEPD, and triangles represent PCD.

Table 2
Model performance statistics of surface concentrations for O_3, NO_2, SO_2, CO, PM_{10}, and $PM_{2.5}$ at north and south part of PSEA and EA in March and April.

1	2	3	4	5	6		7	8	9	10	11	12	13	14	15	16
	PSEA[a]											EA[b]				
	North						South									
	Obs	Sim	NMB (%)	R	[b] of data pairs		Obs	Sim	NMB (%)	R	[b] of data pairs	Obs	Sim	NMB (%)	R	[b] of data pairs
CO (ppbv)																
2006	690.01	803.98	16.52	0.71	139		452.58	455.91	**0.73**[c]	0.61	504	619.56	641.69	3.48	0.73	106
2007	861.72	910.81	5.69	0.72	123		511.79	425.32	**−11.32**	0.66	551	619.17	639.41	3.27	0.68	101
2008	678.43	809.89	19.37	0.63	129		471.11	397.43	**−15.63**	0.64	623	608.36	628.48	3.31	0.77	106
2009	654.26	820.51	21.45	0.67	262		449.27	382.37	**−16.89**	0.71	546	527.49	538.24	2.04	0.74	105
2010	926.95	1137.45	22.71	0.72	254		559.62	496.27	**−19.34**	0.66	624	554.43	566.34	2.15	0.79	105
SO_2 (ppbv)																
2006	1.51	2.18	44.05	0.64	123	4.77		5.12	**7.29**	0.52	399	6.57	8.09	23.25	0.96	257
2007	2.35	2.96	26.19	0.66	120	3.97		4.15	**4.26**	0.53	301	3.67	4.49	22.55	0.97	251
2008	2.81	3.57	27.54	0.71	131	3.85		5.05	**31.15**	0.51	462	4.42	5.38	21.82	0.96	242
2009	2.63	3.82	45.59	0.69	133	3.57		4.97	**39.47**	0.49	368	2.97	3.61	21.57	0.96	268
2010	2.37	3.27	37.98	0.69	155	3.38		5.22	**54.19**	0.51	480	4.73	6.12	29.29	0.98	203
NO_2 (ppbv)																
2006	13.39	14.41	7.58	0.63	122	12.61		11.5	**−9.59**	0.57	540	30.04	36.19	20.46	0.79	167
2007	15.64	17.67	12.96	0.62	102	12.39		8.7	**−29.25**	0.56	457	22.36	28.57	27.77	0.89	208
2008	13.08	14.83	13.33	0.66	126	12.52		8.71	**−30.39**	0.67	534	23.15	30.35	31.09	0.90	177
2009	13.32	15.14	13.65	0.59	165	12.41		7.64	**−38.41**	0.61	424	19.47	25.71	32.02	0.90	180
2010	15.69	17.81	13.59	0.61	165	13.39		8.5	**−36.49**	0.57	468	21.46	27.81	29.57	0.92	186
O_3 (ppbv)																
2006	30.69	38.31	24.82	0.69	409	26.1		30.39	**16.45**	0.67	192	47.97	45.84	−4.43	0.78	677
2007	37.13	43.75	17.82	0.63	383	29.98		38.29	**27.68**	0.76	186	50.07	45.94	−8.26	0.77	664
2008	37.18	46.81	25.89	0.63	423	28.47		39.2	**37.67**	0.82	193	49.36	46.81	−5.18	0.77	621
2009	34.23	44.61	30.03	0.86	405	27.83		37.07	**33.17**	0.8	216	47.59	46.72	−1.83	0.77	660
2010	41.68	54.17	29.96	0.66	447	32.72		45.75	**39.95**	0.86	155	43.76	42.19	−3.58	0.76	640
PM_{10} ($\mu g/m^3$)																
2006	47.07	37.19	−20.98	0.83	100	29.19		16.25	**−44.32**	0.84	183	111.84	45.31	−59.49	0.54	4789
2007	81.3	51.06	−37.04	0.92	181	36.53		20.08	**−45.04**	0.7	186	91.78	45.64	−50.27	0.48	4719
2008	69.95	50.12	−28.34	0.81	174	32.22		16.38	**−49.16**	0.88	207	95.95	47.09	−50.92	0.51	4663
2009	101.05	67.03	−33.67	0.89	158	34.14		15.76	**−53.83**	0.91	158	89.35	46.78	−47.64	0.54	4887
2010	117.95	78.46	−33.48	0.85	186	40.05		20.22	**−49.52**	0.82	213	89.92	41.95	−53.35	0.53	4682
$PM_{2.5}$ ($\mu g/m^3$)																
2006												42.12	34.51	−18.07	0.83	118
2007												34.99	33.62	−3.89	0.85	119
2008												43.95	37.09	−15.68	0.83	117
2009												30.29	29.64	−2.23	0.82	120
2010												31.86	27.9	−12.45	0.81	120

[a] Observations used for PSEA evaluation include O_3, CO, SO_2, NO_2, and PM_{10} from PCD, and O_3, NO_2, SO_2, PM_{10} from EANET stations within PSEA.
[b] Observations used for EA evaluation include PM_{10}, SO_2, NO_2derived from 6 cities of API in China, PM_{10} derived from 86 cities of China, O_3, CO, SO_2, NO_2, PM_{10}, $PM_{2.5}$ from TAQMN super sites, O_3, CO, SO_2, NO_2, $PM_{2.5}$ from HKEPD, and O_3, SO_2, NO_2, PM_{10} from EANET stations within EA.
[c] Bold NMB values indicated increasing model discrepancy from 2006 to 2010.

from 27.7% in 2007 to 39.9% in 2010. Evaluation for PM_{10} over south PSEA showed consistent underestimation by −53.8%–44.3% with no obvious temporal trend found. And according to Table 2, almost all pollutants concentrations were found increase from 2006 to 2010 as indicated by the observations. The concentrations of CO, NO_2, O_3, and PM_{10} increased from 452.6 ppbv, 11.5 ppbv, 26.1 ppbv and 16.3 $\mu g/m^3$ in 2006 respectively to 559.6 ppbv, 13.4 ppbv, 32.7 ppbv, and 40.1 $\mu g/m^3$ in 2010 respectively. As no significant annual variation of meteorology was found during 2006–2010 (shown in Table S2), this increasing trend indicated that anthropogenic emission within the PSEA countries may have substantial growth after year 2006, thus the emission inventory was lag behind. Since south part of PSEA was controlled by anthropogenic emission which was represented by INTEX-B in this study, the distinct temporal trend of model performance should be attributed to the uncertainties within INTEX-B inventory. The INTEX-B inventory was developed for year 2006 thus resulted in increasing simulation bias in simulation from year to year.

For evaluation over EA, model performance was found consistent during different years, CMAQ overpredicted CO, SO_2, and NO_2 with NMB values of 2%–3.5%, 21.6%–29.3%, 20.5%–32% respectively, and underpredicted O_3, $PM_{2.5}$, and PM_{10} with NMB values of −8.3%–1.8%, −18%–2.3%, and −47.6%–59.5 respectively. Despite that PM_{10} was underestimated significantly due to the impact from dust storms which will be discussed in Section 3.2.3, no significant annual trend was found for the model performance evaluation.

As mentioned in Section 2.1, within the simulation domain China's emission data was from Zhao et al. (2013a) which has been consistently updated. INTEX-B was applied over both EA countries including Japan and South Korea and PSEA countries for all the 5 simulation years. But based on the annual performance trend shown in Table 2, significant changes of simulation discrepancy from year to year were only found over PSEA, indicating that the anthropogenic emission increased substantially only at PSEA after 2006. The emission over Japan and South Korea may not change much because the modeling discrepancies remain in similar level for different years with same set of inventory, and observations at EA also indicated the pollutants concentrations remain similar for different years at Japan and South Korea. To verify the implications about emission uncertainties by the evaluation statistics, we examined the CO_2 emission as an indicator for PSEA and EA (Japan and South Korea) to investigate their annual variation as shown in Fig. 3.

CO_2 emission data was from World Bank (http://datacatalog.worldbank.org/). For EA countries Japan and South Korea, annual CO_2 emission was generally constant between 1700 and 1705 M

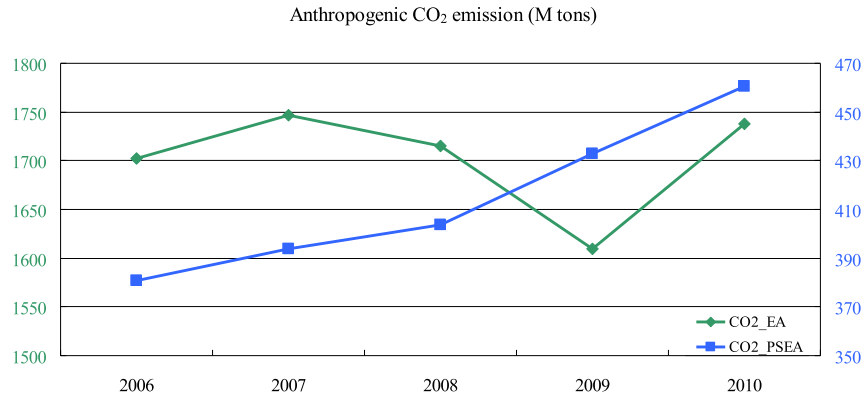

Fig. 3. Annual anthropogenic CO_2 emission for EA (green line: Japan and South Korea) and PSEA (blue line: Thailand, Myanmar, Vietnam, Laos, and Cambodia). (For interpretation of the references to color in this figure legend, the reader is referred to the web version of this article.)

tons (1E6 tons) except for 2009, which was due to the impact of global economic recession starting from the second half year of 2008. While for PSEA on the other hand, anthropogenic CO_2 emission increased monotonically during this period and 2010 emission was about 21% higher than that in 2006. The different annual trends of CO_2 emission indicated that although INTEX-B was applied for both EA (Japan and South Korea) and PSEA countries, the real anthropogenic emission over PSEA should have significant growth while the emission over EA changed slowly. So the relatively better CMAQ performance in 2006 and worse performance for other years over south PSEA should mainly due to the outmoded anthropogenic emission, and the comparison between PSEA and EA for annual variations of model performance indicated the urgency of updating anthropogenic emission inventory of the south PSEA countries.

3.1.2. Evaluation over PSEA

Table 2 suggested different model performances at north and south PSEA, so in this section we examined the daily variations of air pollutants at two parts of PSEA respectively to explore the different reasons for the simulation discrepancy. Observation for CO was from PCD which all located within Thailand. Despite that biomass burning contributed significantly for CO emission over PSEA during spring time, Huang et al. (2013) demonstrated that only the north part of Thailand was strongly affected since it was close to Myanmar which had the most intensive burning activities, and the southern part contained the two largest seaports and major power plants with most of the industrial facilities (Pham et al., 2007), which was mainly affected by the anthropogenic emissions. Here we selected four sites from different regions: Lampang at north, Ayuthaya at central, Samut Sakorn and Chachoengsao at south Thailand to examine the uncertainties from different inventories. Daily variations of CO from observation and simulation for these sites were summarized as shown in Fig. 4. Temporal variations of CO was reproduced well and model basically captured the peak and bottom values at Lampang, with a consistent slightly overestimation for all 5 years simulation. With a relatively long atmospheric life time, simulation bias for CO at north PSEA was mainly driven by uncertainty within the biomass burning emission since meteorology was reproduced well by WRF. FLAMBE was employed in this study as biomass burning emission inventory, and several studies have suggested it may be overestimated over PSEA: Fisher et al. (2010) reported that FLAMBE emission might be overestimated by a factor of two, and Alvarado et al. (2010) implied that FLAMBE should be reduced by 45% over southeast Asia to match with the observations. Although in this study we also find overestimation of FLAMBE based on the CO evaluation at Lampang, the bias was around 6%–22% as mentioned by statistics shown in Table 2. The 5 year averages of daily CO at Lampang were 703 ppbv and 811 ppbv for observation and simulation respectively, which implied overestimation by 15%. At Ayuthaya located in central Thailand, CO concentration was reproduced well with the observed and simulated values as 608 ppbv and 570 ppbv respectively. At Samut Sakorn and Chachoengsao however, model was found to underpredict CO concentrations. The observed and simulated values are 653.4 ppbv and 442.3 ppbv at Samut Sakron, 366.5 ppbv and 315.7 ppbv at Chachoengsao respectively. Biomass burning usually introduce intensive CO loadings in March and lead to the drastic daily variations of CO concentration as shown at Lampang, thus the relatively flat curves of daily CO at Samut Sakorn and Chacherngsao verified that the southern sites got little impact from biomass burning. Consequently, evaluation at these sites indicated about underestimation of anthropogenic CO emission by 20%–30%.

Besides the systematic errors of the total amount of emission estimation, spatial allocation of the emission into modeling grid cells may also introduce uncertainties. Following the approach suggested by Streets et al. (2003), the INTEX-B used surrogate GIS distributions of population for redistributing emission in case the exact locations of large point sources were not available, which may put anthropogenic emission into incorrect positions. To evaluate the spatial allocation of anthropogenic emission over south PSEA, we further examined the model performance at different sites within southern Thailand. At southern Thailand, EANET had an observational station located at the urban center (13.73°N, 100.56°E) of Bangkok, and PCD have one observational station at the province Samut Prakan (13.59°N, 100.59°E). The locations of these two stations were represented as purple triangles shown in Fig. 5(a). Fig. 5(a) also showed the anthropogenic SO_2 emission from power plants sector within INTEX-B denoted as color contours (emission unit is moles per second per square km). We also used data from Carbon Monitoring for Action (CARMA, http://carma.org/) to identify the real locations of power plants (annual capacity greater or equal to 1E6 MWh) within this area, as denoted by black cycles in Fig. 5(a). CARMA (Wheeler and Ummel, 2008; Ummel K., 2012) is a database containing information about the carbon emissions from worldwide power plants. As shown in Fig. 5(a), there was no large power plant located inside the urban area of Bangkok, but the emission inventory assigned most of the SO_2 emission into the model grid which contains Bangkok city. Power plants locations indicated by CARMA were also consistent with Thailand's local bottom-up inventory reported by Thao et al. (2014). Fig. 5(b) showed the population density (data from LandScan) over this area. It demonstrated that the anthropogenic emission had a very similar spatial distribution pattern as the population density.

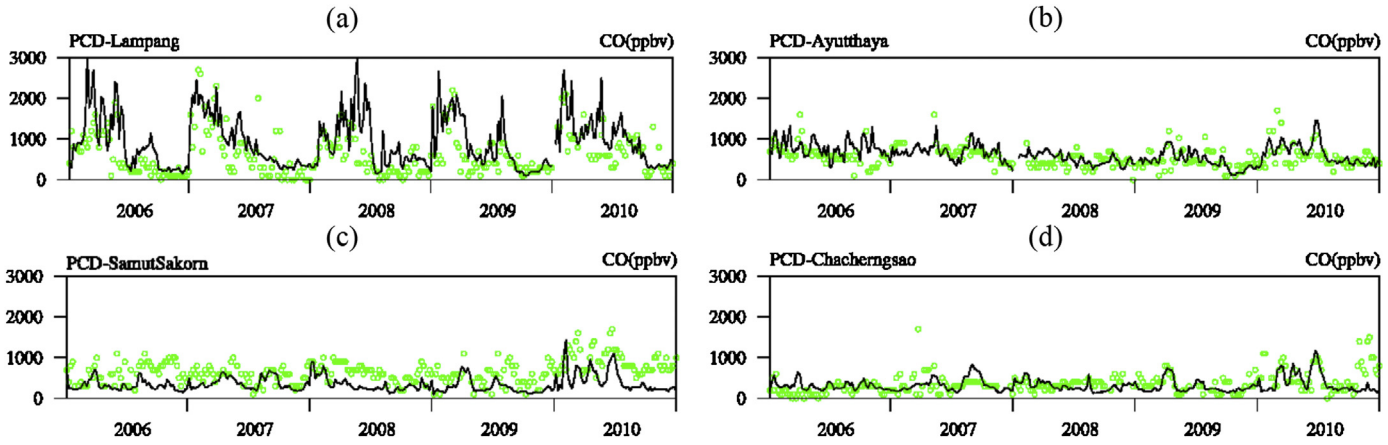

Fig. 4. Temporal variation of daily average CO at (a) Lampang, (b) Ahuthaya, (c) Samut Sakorn, and (d) Chacherngsao, with green markers represented observations and solid black lines indicated CMAQ predictions. (For interpretation of the references to color in this figure legend, the reader is referred to the web version of this article.)

These evidences verified that the spatial allocation of anthropogenic emission based on population distribution introduced bias into the modeling system, which may cause overestimation of emission at highly populated area and underestimation at industrial area with less population.

To demonstrate the uncertainties caused by spatial allocation of anthropogenic emissions, temporal variations of O_3, NO_2, SO_2 and PM_{10} were summarized for the PCD station at Samut Prakan and EANET station at Bangkok as shown in Fig. 6. CMAQ can generally reproduce the concentration and variations of SO_2 at Samut Prakan, but overestimate SO_2 significantly at Bangkok. Average SO_2 concentration from observation and simulation were 4.5 ppbv and 7.3 ppbv respectively at Samut Prakan, and 4.5 ppbv and 20.1 ppbv respectively at Bangkok. Despite similar level of observed SO_2, simulation had substantial larger overestimation at Bangkok than at Samut Prakan although the modeling grid cells were next to each other as shown in Fig. 5(a). Model performance for NO_2 also showed similar comparison between Samut Prakan and Bangkok as demonstrated by Fig. 6(c) and (d): NO_2 at Bangkok was significantly overestimated with averages of observed and simulated values were 12.2 ppbv and 41.2 ppbv respectively, and NO_2 at Samut Prakan was slightly underestimated with averages of observed and simulated values were 17.9 ppbv and 14.9 ppbv respectively. Since industry and transport are the top two contributors for NOx emission, simulation bias may come from these two emission sectors in INTEX-B. For O_3 prediction, model showed smaller discrepancy at Bangkok: the averages of observed and simulated O_3 were 18.2 ppbv and 25.6 ppbv respectively, and the values were 19.2 ppbv and 35.6 ppbv respectively at Samut Prakan. For PM_{10} prediction, simulation was underestimated at both sites but with smaller bias at Bangkok, with the averages of observed and simulated values were 35.2 $\mu g/m^3$ and 25.1 $\mu g/m^3$ respectively, and the values at Samut Prakan were 53.7 $\mu g/m^3$ and 17.6 $\mu g/m^3$ respectively. Since using spatial surrogate of population density resulted in overestimation of emission at Bangkok and underestimation at Samut Prakan, model should have positive bias for all pollutants at Bangkok and negative bias at Samut Prakan if the total emission was started from an accurate benchmark. Thus the results shown by Figs. 5 and 6 suggested that there may exist systematic errors within the INTEX-B for the total emission as well, where SO_2 was

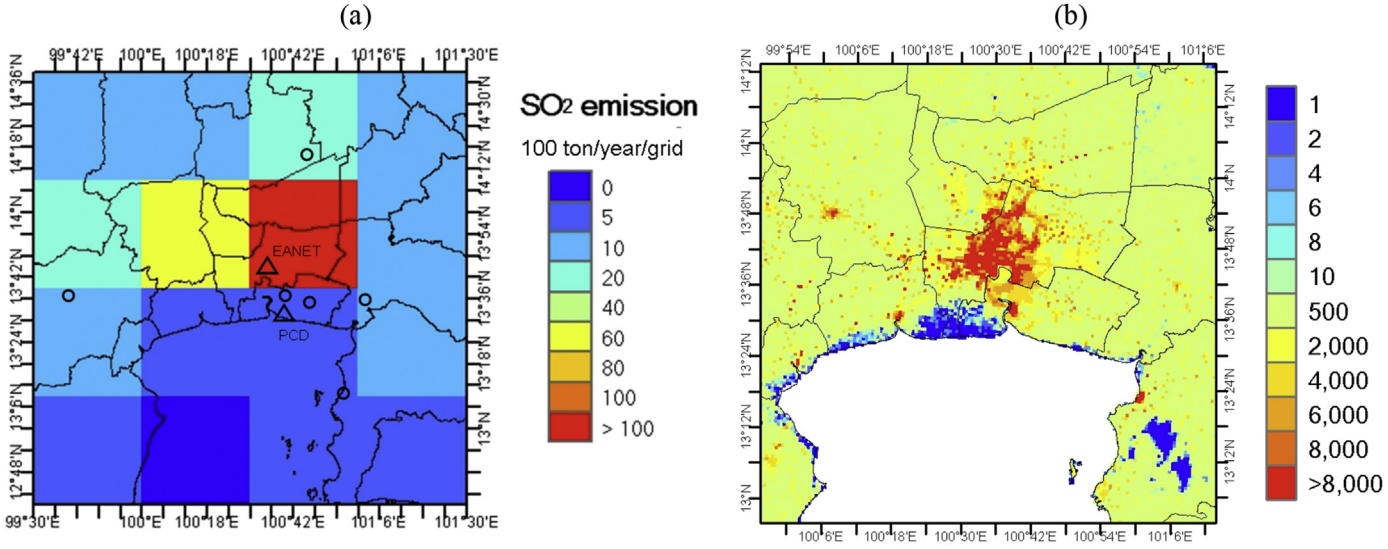

Fig. 5. (a) Spatial distribution of anthropogenic SO_2 emission from power plant sector within INTEX-B (color contours, unit is moles per second per square km), locations of EANET and PCD observational station (triangles), and locations of major power plants with annual capacity larger than 1E6 MWh (cycles); (b) Population density over golf of Thailand area with data from LandScan (LandScan 2006 High Resolution global Population Data Set copyrighted by UT-Battelle, LLC, operator of Oak Ridge National Laboratory.).

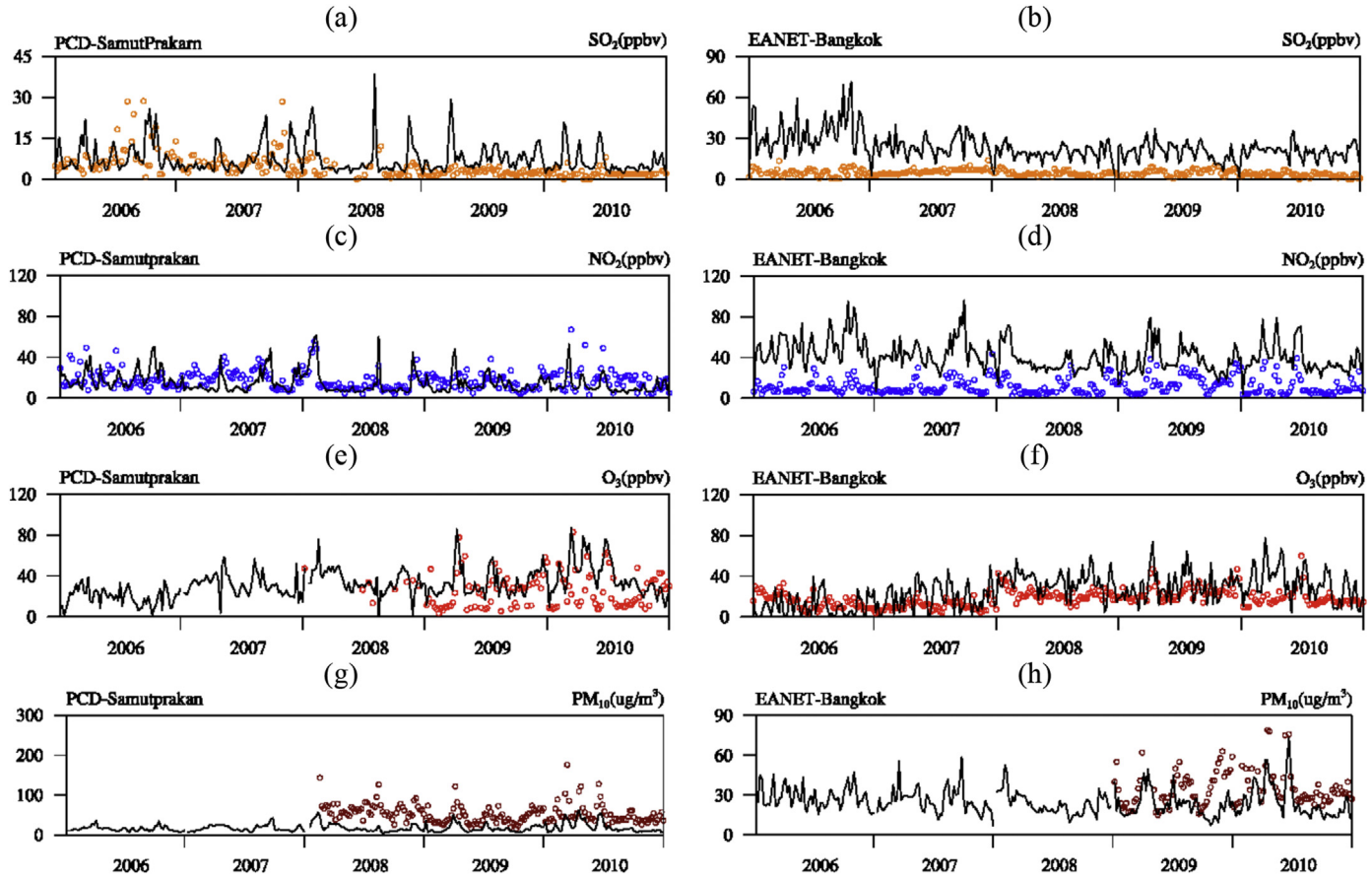

Fig. 6. Temporal variation of daily average SO_2 (1st row), NO_2 (2nd row), O_3 (3rd row), and PM_{10} (4th row) at Samut Prakan (left column) and Bangkok (right column). Markers represent observations and solid black lines indicate CMAQ predictions.

overestimated and PM_{10} was underestimated domain wide, and NO_2 was overestimated at highly populated area but underestimated at rest places.

3.1.3. Evaluation over EA

Although statistics shown in Table 2 demonstrated that there was no significant annual variation of model performance over EA, it also suggested that systematic errors exist as the model consistently overestimated NO_2 and SO_2 by 20%–30% and underestimate PM_{10} by 50%–60% for all the 5 modeling years. So in this section we investigated the uncertainties which should be responsible for the systematic errors over EA. Fig. 7 summarized the temporal changes of daily NO_2, SO_2, and PM_{10} at Beijing, Guangzhou, and Banyu, which were located at the north, south and northeast part of EA. As shown in Fig. 7 (a) and (b), Guangzhou had a much lower PM_{10} concentration than Beijing, and simulation agreed better with observation at this site. The 5-year averages of observed and simulated PM_{10} at Guangzhou were 77.2 $\mu g/m^3$ and 62.9 $\mu g/m^3$ respectively, while the values at Beijing were 152.1 $\mu g/m^3$ and 64.7 $\mu g/m^3$ respectively. Evaluation of PM_{10} at Banyu also showed large underestimation, the values for observation and simulation were 31.9 $\mu g/m^3$ and 14.3 $\mu g/m^3$ respectively. Guangzhou was located at southern China where anthropogenic source was the dominant contributor for PM_{10}, thus Fig. 7(b) suggested a reasonable good accuracy of the anthropogenic emission. For Beijing and Banyu on the other hand, larger underestimation should be attributed to the impacts of dust storm. Spring time dust storm from Taklimakan and Gobi desert in EA have been demonstrated by many studies to have dominant impact on the elevated PM_{10} levels over north part of China and the influence can reach oversea to Japan (Onishi et al., 2012; Shimizu et al., 2014; Watanabe et al., 2014). Table 2 suggested that 2006 and 2010 had the largest underestimated PM10 for EA, which were also the two years with most frequent dust storms during this period (Yang et al., 2013). Based on our evaluation the dust emission was not well represented in the modeling system. Although the recent version of CMAQ v5.0.1 was developed with a new plume rise scheme to quantify the eolian dust emission (Appel et al., 2013), it lacked thoroughly validation for application over EA due to limited observations and modeling studies. As Fu et al. (2014) reported that the default friction velocity threshold should be reduced by half in order to drive the model to generate enough dust particles to agree with observation, the underestimated dust emission within CMAQ would be the most possible reason for underprediction of total PM10 at north EA. For SO_2 evaluation, CMAQ can generally reproduce the temporal variations of SO_2 with moderate overestimation at Beijing and minor underestimation at Guangzhou as shown in Fig. 7 (d) and (e). Although no significant temporal trend was found for SO_2 evaluation in EA based on evaluation statistics shown in Table 2, NMB value was found slightly larger in 2010 (29.3%) than that in 2006 (23.3%), and the temporal variations of SO_2 in Beijing also indicated larger discrepancy in 2009 and 2010. China started to reduce SO_2 emission during the 11th five-year-plan from 2006 to 2010 (The Sate Council of the People's Republic of China 2011), and the inventory may not timely represent all the deductions as implementation of control technologies have large regional and temporal variations. This should be responsible for the overall 20%–30% overestimation over China and larger bias in

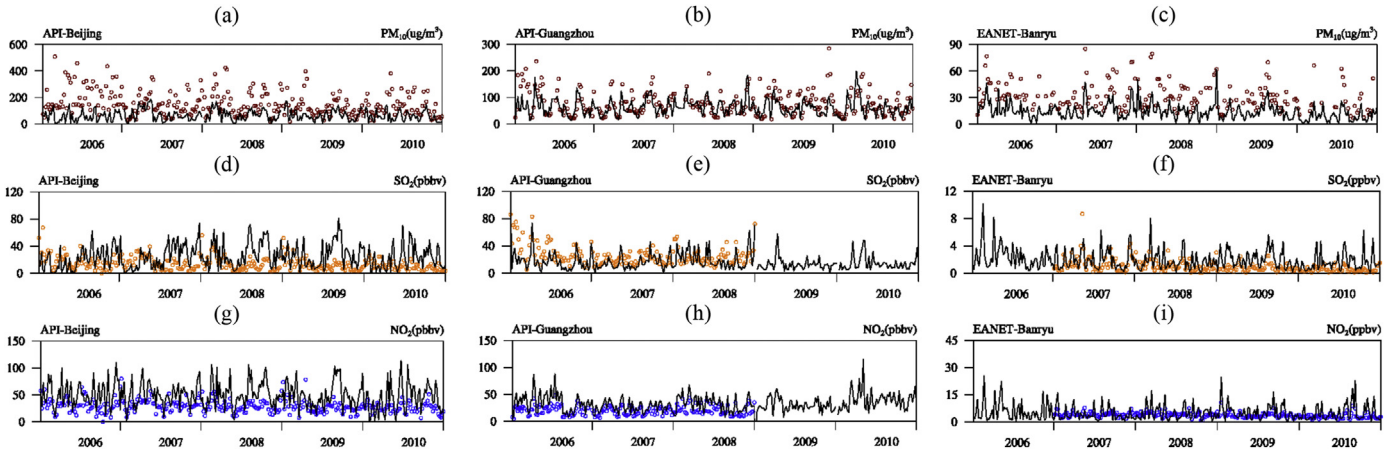

Fig. 7. Temporal variations of daily average PM_{10} (1st row), SO_2 (2nd row), and NO_2 (3rd row) at Beijing (left column), Guangzhou (middle column), and Banyu (right column). Markers represent observations, solid black lines indicate CMAQ predictions.

metropolitan area such as Beijing. NO_2 was overestimated by about 40% at both Beijing and Guangzhou as shown in Fig. 7 (g) and (h), consistent with the evaluation statistics shown in Table 2. The overestimation of NO_2 suggested that NO_x emission might be overestimated, yet more observation data for total nitrogen oxide compounds(NOy) would is needed to further verify this in future study. For evaluation at Banyu, model can capture daily changes of SO_2 and NO_2 well with some minor overestimations during 2007 as shown in Fig. 7(f) and (i). Biases between observation and simulation were getting larger from 2007 to 2010 and observations showed slightly decrease concentrations for both SO_2 and NO_2, suggesting the INTEX-B emission applied over Japan also needs updated for these species.

3.2. Evaluation for column densities

Vertical column density (VCD) of NO_2 and AOD were also evaluated to examine the model performance for predicting vertical distribution and transport of pollutants and aerosol properties. Monthly average tropospheric VCD of NO_2 was evaluated with satellite retrieval from OMI as shown in Fig. 8, and evaluation statistics were calculated for north and south part of PSEA respectively, as shown in Table 3. Considering the satellite's descending nodes at local time, CMAQ outputs at 14:00 Beijing Time (BT) were selected for NO_2 to make them comparable with satellite product. Despite the overall good agreement between simulation and OMI retrieval, large overestimation was found over north part of PSEA as shown by Fig. 8. The spatial distributions of tropospheric VCD NO_2 shown in Fig. 8 suggested that the overestimation over north part of PSEA should be attributed to uncertainty within biomass burning emission. According to Table 3, south PSEA was found to have underestimation of VCD NO_2 with NMB values of −32%–11% which was consistent with the surface NO_2 evaluation discussed in Section 3.2, and north PSEA was found to have larger overestimation with NMB values of 37%–49%. Biomass burning NO_x emission was derived based on emission factor which specify the amount of emitted NO_x per unit of dry matter consumed. In this study we used the emission factors from Akagi et al. (2011), which were derived based on in situ measurements for different types of fire with no seasonal or regional changes. But recently Castellanos et al. (2014) used OMI observations and reported that NO_x emission factor had substantial spatiotemporal variability, and for deforestation fire in dry season the emission factor was about 10%–46% less than the values reported by Akagi et al. (2011). As deforestation was the most significant fire over north PSEA (Reid et al., 2009), the overestimated NO_x emission factor should be responsible for the overestimation of VCD NO_2. Model prediction over EA have NMB values of 0.8%–4.4%, indicating minor overestimation of NO_2 which was also consistent with the surface evaluation.

AOD was evaluated with both satellite retrievals from MODIS and ground measurements from AERONET. To make CMAQ predictions comparable with MODIS AOD, simulations were extracted for 11:00 BT which was the descending time for Terra satellite carrying MODIS, and daily averages from simulation were used for comparison with AERONET. Fig. 9 demonstrated the comparison of monthly average AOD between MODIS and CMAQ. Spatial distributions of AOD showed good agreement between simulation and satellite retrieval, and overlays of CMAQ and AERONET showed similar evaluation results as summarized in Figure S2 and S3. Over EA, high AOD values were found over North China Plain, Pear River Delta, and Yangtze River Delta due to the intensive anthropogenic emissions within these industrial areas. High AOD values were also found over southwest of China and north part of PSEA due to impact from biomass burning. Unlike the evaluation of VCD NO_2 which showed better performance at south PSEA due to overestimated biomass burning NO_x emission factor at north PSEA, the evaluation of AOD with both MODIS retrievals and AERONET measurements indicated better performance at the north PSEA as shown by the statistics in Table 4. For evaluation based on MODIS retrievals, north part of PSEA has higher AOD with the observed and simulation values are 0.52–0.71 and 0.42–0.59 respectively. Moderate underestimation at north PSEA was −16%–21% with no significant annual trend found. South part of PSEA had much lower AOD level, with observed and simulated values were 0.29–0.37 and 0.12–0.21 respectively, and the underestimation are more severe with NMB values of −62%–46%. Evaluation based on AERONET measurements show higher concentrations of AOD as compared to MODIS retrievals for both north and south part of PSEA, but the NMB values are fairly consistent with evaluation based on MODIS, which also shows underestimation of −28%–14% and −66%–43% at north and south PSEA respectively. As an important precursor for secondary inorganic aerosols, both surface and column density of NO_2 were underestimated at south PSEA, which should be partly responsible for the large underestimation of AOD at south part of PSEA. But as many modeling studies (Fu et al., 2012; Wang et al., 2011; Zhao et al., 2013a) suggested the CMAQ usually underestimated AOD over Asia, it's essential to have more research efforts to quantify the uncertainty from emission and also the uncertainty within the model itself.

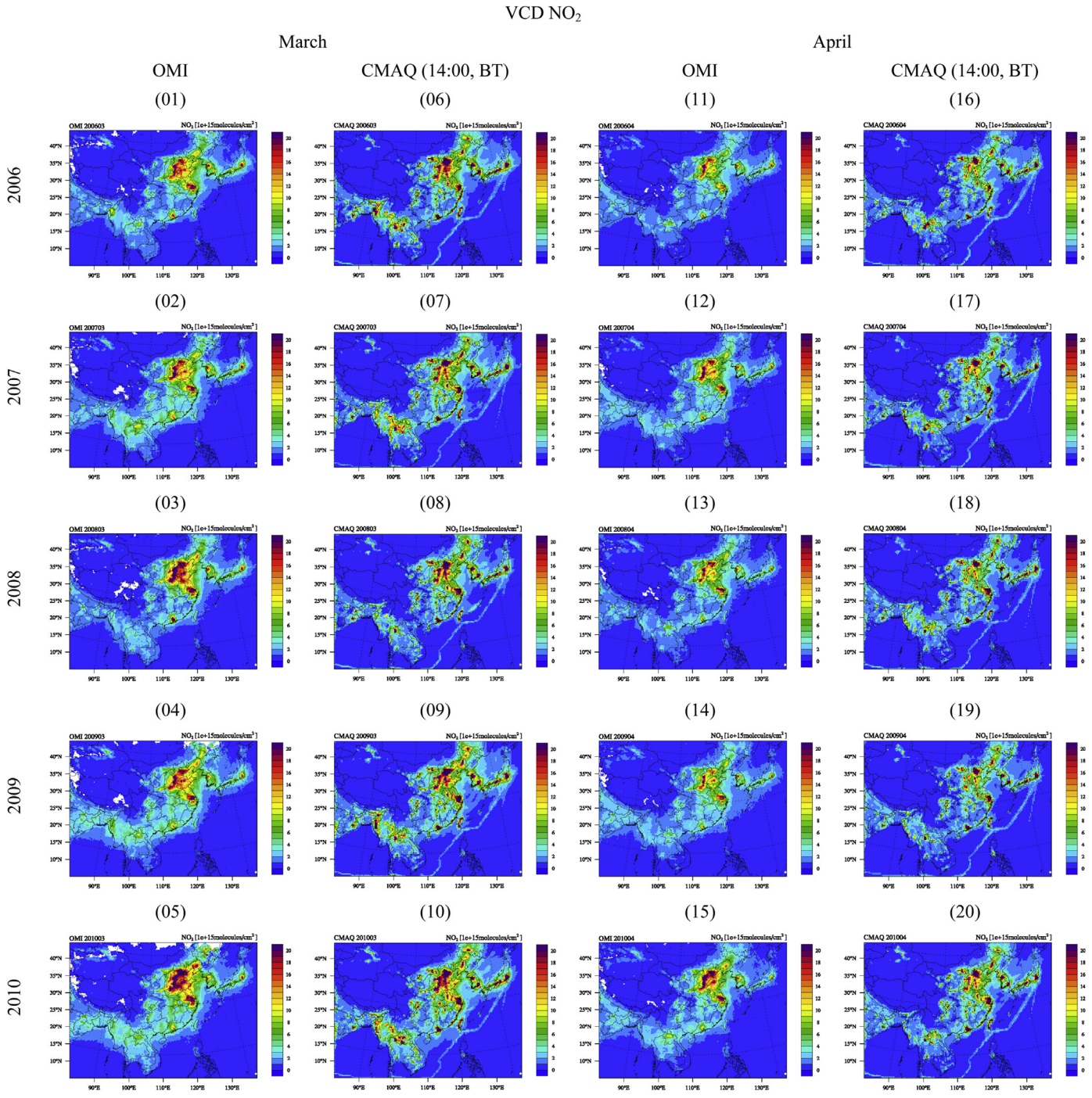

Fig. 8. Comparison of monthly average VCD of NO_2 from OMI and CMAQ (14:00, BT).

4. Conclusions

In this study, WRFv3.4/CMAQv5.0.1 was applied over PSEA and EA and was thoroughly evaluated with observations from multiple networks and satellite retrievals. This is the first study incorporating multi-year WRF/MCAQ simulations over PSEA and EA focusing on the biomass burning period, and results from this study provide essential assessment for probing into the possible uncertainties within the modeling system. Although modeling applications over PSEA and EA have been performed in some recent studies, understanding about the driving forces of simulation discrepancy was poorly developed due to the large unknown bias within both biomass burning and anthropogenic emission. In this study based on evaluation with measurements and other analysis data from World Bank, CARMA, and LandScan, we found spatio-temporal variations of the systematic bias and identified different factors responsible for the simulation discrepancy. These findings are summarized as below:

(1). Evaluation at north PSEA (>17°N) suggested systematic overestimation of biomass burning CO emission by 6%–23% and NO_2 by 8%–14% in the surface layer and 40%–50% for the

Table 3
Model performance statistics of VCD NO_2 for north and south part of PSEA and EA with observations from OMI.

	PSEA								EA			
	North				South							
	Obs[a]	Sim	NMB (%)	R	Obs	Sim	NMB (%)	R	Obs	Sim	NMB (%)	R
2006	1.08	1.51	39.63	0.61	0.61	0.54	−11.62	0.89	1.57	1.64	4.44	0.85
2007	1.26	1.73	37.11	0.64	0.61	0.45	−24.59	0.87	1.69	1.71	0.79	0.83
2008	1.09	1.53	40.44	0.61	0.61	0.48	−20.18	0.88	1.65	1.72	4.19	0.84
2009	1.25	1.83	46.32	0.62	0.59	0.44	−25.58	0.87	1.73	1.81	4.27	0.84
2010	1.29	1.92	49.02	0.64	0.59	0.41	−32.77	0.87	1.91	1.93	1.61	0.87

[a] Unit for observations and simulations are 1E15 molecules/cm.^{2}.

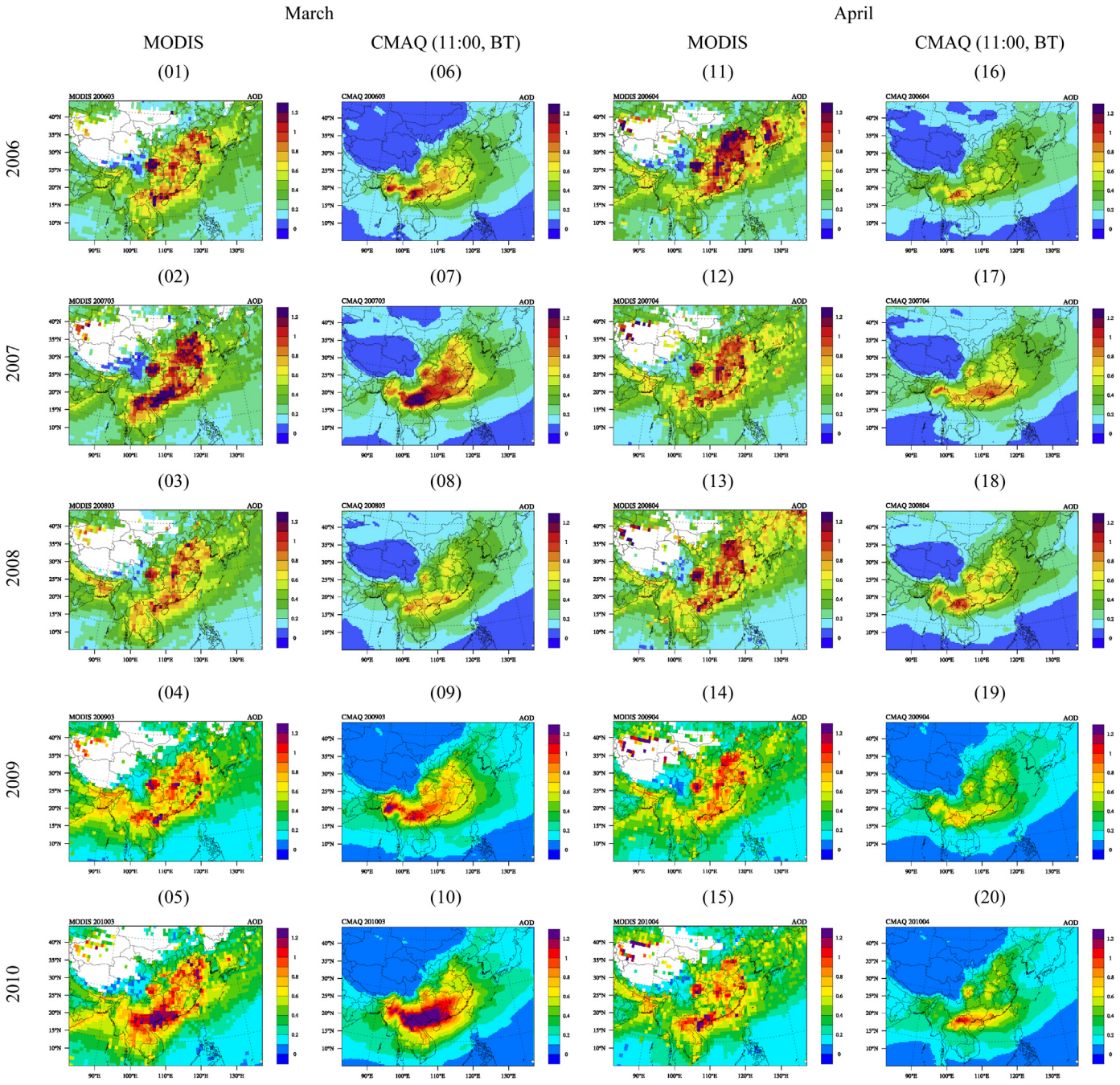

Fig. 9. Comparison of monthly average AOD from MODIS and CMAQ (11:00, BT).

Table 4
Model performance statistics of AOD for north and south part of PSEA and EA with observations from MODIS and AERONET.

	PSEA								EA			
	North				South							
	Obs	Sim	NMB (%)	R	Obs	Sim	NMB (%)	R	Obs	Sim	NMB (%)	R
AOD (observation from MODIS)												
2006	0.52	0.42	−19.84	0.84	0.37	0.21	−46.19	0.92	0.41	0.21	−48.22	0.87
2007	0.62	0.49	−21.36	0.82	0.32	0.13	−58.82	0.87	0.41	0.26	−38.32	0.89
2008	0.57	0.45	−20.33	0.85	0.36	0.15	−57.49	0.89	0.41	0.23	−43.45	0.91
2009	0.62	0.49	−20.83	0.75	0.29	0.12	−59.87	0.87	0.39	0.21	−47.99	0.83
2010	0.71	0.59	−15.75	0.89	0.31	0.12	−62.13	0.81	0.39	0.21	−47.53	0.85
AOD (observation from AERONET)												
2006	0.65	0.46	−24.42	0.79	0.59	0.34	−42.69	0.87	0.61	0.34	−44.96	0.74
2007	0.78	0.56	−28.35	0.82	0.57	0.22	−62.21	0.71	0.61	0.44	−27.87	0.86
2008	0.91	0.78	−14.16	0.76	0.57	0.29	−49.92	0.84	0.53	0.38	−26.83	0.83
2009	0.81	0.67	−16.67	0.81	0.41	0.19	−53.43	0.81	0.55	0.31	−44.08	0.77
2010	1.21	0.93	−23.13	0.91	0.53	0.18	−65.97	0.35	0.42	0.29	−30.69	0.78

tropospheric column density. Comparing with the most recent study by Castellanos et al. (2014), NO_x emission factor was overestimated by up to 46% in this study for the deforestation fire, which should be responsible for the bias of NO_2 simulation.

(2). Evaluation at south PSEA ($\leq$17°N) suggested significant errors within the anthropogenic emission in terms of both total intensity and spatial allocation. Evaluation statistics for year 2006 suggested the INTEX-B emission contains minor bias for NO_2 and SO_2 by ±10%, but both surface observations and World Bank data demonstrated substantial growth of pollutants concentrations and anthropogenic emissions from 2006 to 2010, thus the outmoded INTEX-B will cause increasing model discrepancy if applied for simulation years after 2006. Comparing with power plants locations data from CARMA, spatial allocation of anthropogenic emission based on population distribution introduced large bias by overestimating emission at highly populated area.

(3). Evaluation at EA suggested significant underestimation of PM_{10} by around 50% over north China and Japan, which should be due to the insufficient dust plume rise within CMAQ, yet more detailed sub-species measurement of PM10 is needed to further verify that underestimation of PM10 is mainly driven by low prediction of dust in the model. CMAQ was found to have moderate overestimation for surface NO_2 and SO_2 by 20%–30%, moderate underestimation for AOD by 30%–50%, minor overestimation for CO by 3.5%, and minor underestimation for O_3 by −9%. Both the signs and values of NMB values are self-consistent for each species over different simulation years, indicating the possible constant systematic bias within the emission inventory over China.

Despite some significant bias found from the simulations, modeling is still one of the most popular approaches for studying air quality and regional climate over PSEA and EA, and is probably the only option for predicting the long-term impacts by biomass burning or anthropogenic activity under different future scenarios. Thus evaluation of retrospective simulations as in this study is essential for understanding the model's discrepancy before applying it for any analysis. Evaluation of chemical transport model (CTM) such as CMAQ need to be very carefully interpreted to help improve the model's capability and accuracy, since uncertainties could be generated from different sources such as different emission categories and parameterization of chemical/physical schemes. As limited observations are available especially for PSEA countries, utilizing different datasets such as satellite retrievals, statistical data from World Bank, CARMA, LandScan and other resources are necessary to facilitate the evaluation process. It is important to notice that besides the systematic errors identified in this study, large uncertainties remain in some other key aspects which may cause model discrepancy as well, such as the uncertainty of injection height of biomass burning plume, emission factors for different species and different fire types and so on. And the even more important issue is, how can these uncertainties be reduced to enable the model to provide more reliable predictions. Based on the findings from this study, we would suggest updating and refining the spatial allocation of anthropogenic emission and regular local measurements over PSEA as the most urgent research efforts due to its significant impact on model performance. Improving the plume rise scheme of mineral dust within CMAQ would be another important topic for model development and application over EA.

Acknowledgment

We thank NASA GSFC on funding support (grant No.: NNX09AG75G). We would like to acknowledge Edward J. Hyer for providing biomass burning emission. We thank Dr. Keiichi Sato and Dr.Ayako Aoyagi from Asia Center for Air Pollution Research for providing the EANET data. We also would like to acknowledge Thailand PCD, China MEP, Taiwan EPA and CWB, Hong Kong EPD for providing the observation data, and thank NASA for providing AERONET, OMI, MODIS, and LIS/OTD data. We thank National Institute for Computational Sciences (NICS) for providing the computer sources for model simulations of this research.

Appendix A. Supplementary data

Supplementary data related to this article can be found at http://dx.doi.org/10.1016/j.atmosenv.2015.06.026.

References

Akagi, S.K., Yokelson, R.J., Wiedinmyer, C., Alvarado, M.J., Reid, J.S., Karl, T., Crounse, J.D., Wennberg, P.O., 2011. Emission factors for open and domestic biomass burning for use in atmospheric models. Atmos. Chem. Phys. 11, 4039–4072.

Alvarado, M.J., Logan, J.A., Mao, J., Apel, E., Riemer, D., Blake, D., Cohen, R.C., Min, K.E., Perring, A.E., Browne, E.C., Wooldridge, P.J., Diskin, G.S., Sachse, G.W., Fuelberg, H., Sessions, W.R., Harrigan, D.L., Huey, G., Liao, J., Case-Hanks, A., Jimenez, J.L., Cubison, M.J., Vay, S.A., Weinheimer, A.J., Knapp, D.J., Montzka, D.D., Flocke, F.M., Pollack, I.B., Wennberg, P.O., Kurten, A., Crounse, J., St Clair, J.M., Wisthaler, A., Mikoviny, T., Yantosca, R.M., Carouge, C.C., Le Sager, P., 2010. Nitrogen oxides and PAN in plumes from boreal fires during ARCTAS-B and their impact on ozone: an integrated analysis of aircraft and satellite observations. Atmos. Chem. Phys. 10, 9739–9760.

Appel, K.W., Pouliot, G.A., Sarwar, G., Pye, H.O.T., Napelenok, S.L., Akhtar, F., Roselle, S., 2013. Evaluation of dust and trace medal estimates from the Community Multiscale Air Quality (CMAQ) model version 5.0. Geosci. Model Dev. 6, 883–899.

Byun, D., Schere, K.L., 2006. Review of the governing equations, computational algorithms, and other components of the models-3 Community Multiscale Air Quality (CMAQ) modeling system. Appl. Mech. Rev. 59, 51–77.

Carmichael, G.R., Sakurai, T., Streets, D., Hozumi, Y., Ueda, H., Park, S.U., Fung, C., Han, Z., Kajino, M., Engardt, M., Bennet, C., Hayami, H., Sartelet, K., Holloway, T., Wang, Z., Kannari, A., Fu, J., Matsuda, K., Thongbooncho, N., Amann, M., 2008. MICS-Asia II: the model intercomparison study for Asia Phase II methodology and overview of findings. Atmos. Environ. 42, 3468–3490.

Castellanos, P., Boersma, K.F., van der Werf, G.R., 2014. Satellite observations indicate substantial spatiotemporal variability in biomass burning NOx emission facotrs for South America. Atmos. Chem. Phys. 14, 3929–3943.

Chuang, M.T., Chou, C.C.K., Sopajaree, K., Lin, N.H., Wang, J.L., Sheu, G.R., Chang, Y.J., Lee, C.T., 2013. Characterization of aerosol chemical properties from near-source biomass burning in the northern Indochina during 7-SEAS/Dongsha experiment. Atmos. Environ. 78, 72–81.

Deng, X.J., Tie, X.X., Zhou, X.J., Wo, D., Zhong, L.J., Tan, H.B., Li, F., Huang, X.Y., Bi, X.Y., Deng, T., 2008. Effects of Southeast Asia biomass burning on aerosols and ozone concentrations over the Pearl River Delta (PRD) region. Atmos. Environ. 42, 8493–8501.

Dong, X.Y., Li, J., Fu, J.S., Gao, Y., Huang, K., Zhuang, G.S., 2014. Inorganic aerosols responses to emission changes in Yangtze River Delta, China. Sci. Total Environ. 481, 522–532.

EANET, 2007. EANET Data Report 2006. Acid Deposition Monitoring Network in East Aisa (EANET).

Fisher, J.A., Jacob, D.J., Purdy, M.T., Kopacz, M., Le Sager, P., Carouge, C., Holmes, C.D., Yantosca, R.M., Batchelor, R.L., Strong, K., Diskin, G.S., Fuelberg, H.E., Holloway, J.S., Hyer, E.J., McMillan, W.W., Warner, J., Streets, D.G., Zhang, Q., Wang, Y., Wu, S., 2010. Source attribution and interannual variability of Arctic pollution in spring constrained by aircraft (ARCTAS, ARCPAC) and satellite (AIRS) observations of carbon monoxide. Atmos. Chem. Phys. 10, 977–996.

Fu, J.S., Jang, C.J., Streets, D.G., Li, Z.P., Kwok, R., Park, R., Han, Z.W., 2008. MICS-Asia II: modeling gaseous pollutants and evaluating an advanced modeling system over East Asia. Atmos. Environ. 42, 3571–3583.

Fu, J.S., Hsu, N.C., Gao, Y., Huang, K., Li, C., Lin, N.H., Tsay, S.C., 2012a. Evaluating the influences of biomass burning during 2006 BASE-ASIA: a regional chemical transport modeling. Atmos. Chem. Phys. 12, 3837–3855.

Fu, J.S., Dong, X.Y., Gao, Y., Wong, D.C., Lam, Y.F., 2012b. Sensitivity and linearity analysis of ozone in East Asia: the effects of domestic emission and intercontinental transport. J. Air & Waste Manag. Assoc. 62.

Fu, X., Wang, S.X., Cheng, Z., Xing, J., Zhao, B., Wang, J.D., Hao, J.M., 2014. Source, transport and impacts of a heavy dust event in the Yangtze River Delta, China, in 2011. Atmos. Chem. Phys. 14, 1239–1254.

Guenther, A., Karl, T., Harley, P., Wiedinmyer, C., Palmer, P.I., Geron, C., 2006. Estimates of global terrestrial isoprene emissions using MEGAN (Model of Emissions of Gases and Aerosols from Nature). Atmos. Chem. Phys. 6, 3181–3210.

Gustafsson, O., Krusa, M., Zencak, Z., Sheesley, R.J., Granat, L., Engstrom, E., Praveen, P.S., Rao, P.S.P., Leck, C., Rodhe, H., 2009. Brown clouds over South Asia: biomass or fossil fuel combustion? Science 323, 495–498.

Holben, B.N., Tanre, D., Simrnov, A., Eck, T.F., Slutsker, I., Abuhassan, N., Newcomb, W.W., Schafer, J.S., Chatenet, B., Lavenu, F., Kaufman, Y.J., Castel, J.V., Setzer, A., Markham, B., Clark, D., Frouin, R., Halthore, R., Karneli, A., O'Neill, N.T., Pietras, C., Pinker, R.T., Voss, K., Zibordi, G., 2001. An emerging ground based aerosol climatology: aerosol optical depth from AERONET. Geophys Res. Lett. 106, 12067–12097.

Hsu, N.C., Herman, J.R., Tsay, S.C., 2003. Radiative impacts from biomass burning in the presence of clouds during boreal spring in southeast Asia. Geophys. Res. Lett. 30.

Huang, K., Fu, J.S., Hsu, N.C., Gao, Y., Dong, X.Y., Tsay, S.C., Lam, Y.F., 2013. Impact assessment of biomass burning on air quality in Southeast and East Asia during BASE-ASIA. Atmos. Environ. 78, 291–302.

Huang, K., Fu, J.S., Gao, Y., Dong, X.Y., Zhuang, G.S., Lin, Y.F., 2014. Role of sectoral and multi-pollutant emission control strategies in improving atmospheric visibility in the Yangtze River Delta, China. Environ. Pollut. 184, 426–434.

Jacob, D.J., Crawford, J.H., Kleb, M.M., Connors, V.S., Bendura, R.J., Raper, J.L., Sachse, G.W., Gille, J.C., Emmons, L., Heald, C.L., 2003. Transport and Chemical Evolution over the Pacific (TRACE-P) aircraft mission: Design, execution, and first results. J. Geophys. Res.-Atmos. 108, 1–19.

Kwok, R.H.F., Fung, J.C.H., Lau, A.K.H., Fu, J.S., 2010. Numerical study on seasonal variations of gaseous pollutants and particulate matters in Hong Kong and Pearl River Delta Region. J. Geophys. Res. 115, D16308. http://dx.doi.org/10.1029/2009JD012809.

Lam, Y.F., Fu, J.S., 2009. A novel downscaling technique for the linkage of global and regional air quality modeling. Atmos. Chem. Phys. 9, 9169–9185.

Lamsal, L.N., Martin, R.V., van Donkelaar, A., Celarier, E.A., Bucsela, E.J., Boersma, K.F., Dirksen, R., Luo, C., Wang, Y., 2010. Indirect validation of tropospheric nitrogen dioxide retrieved from the OMI satellite instrument: Insight into the seasonal variation of nitrogen oxides at northern midlatitudes. J. Geophys. Res.-Atmos. 115.

Li, C., Tsay, S.C., Hsu, N.C., Kim, J.Y., Howell, S.G., Huebert, B.J., Ji, Q., Jeong, M.J., Wang, S.H., Hansell, R.A., Bell, S.W., 2013. Characteristics and composition of atmospheric aerosols in Phimai, central Thailand during BASE-ASIA. Atmos. Environ. 78, 60–71.

Lin, N.H., Tsay, S.C., Maring, H.B., Yen, M.C., Sheu, G.R., Wang, S.H., Chi, K.H., Chuang, M.T., Ou-Yang, C.F., Fu, J.S., Reid, J.S., Lee, C.T., Wang, L.C., Wang, J.L., Hsu, C.N., Sayer, A.M., Holben, B.N., Chu, Y.C., Nguyen, X.A., Sopajaree, K., Chen, S.J., Cheng, M.T., Tsuang, B.J., Tsai, C.J., Peng, C.M., Schnell, R.C., Conway, T., Chang, C.T., Lin, K.S., Tsai, Y.I., Lee, W.J., Chang, S.C., Liu, J.J., Chiang, W.L., Huang, S.J., Lin, T.H., Liu, G.R., 2013. An overview of regional experiments on biomass burning aerosols and related pollutants in Southeast Asia: from BASE-ASIA and the Dongsha Experiment to 7-SEAS. Atmos. Environ. 78, 1–19.

Lu, Z., Zhang, Q., Streets, D.G., 2011. Sulfur dioxide and primary carbonaceous aerosol emissions in China and India, 1996–2010. Atmos. Chem. Phys. 11, 9839–9864.

Muller, J.F., Stavrakou, T., Wallens, S., De Smedt, I., Van Roozendael, M., Potosnak, M.J., Rinne, J., Munger, B., Goldstein, A., Guenther, A.B., 2008. Global isoprene emissions estimated using MEGAN, ECMWF analyses and a detailed canopy environment model. Atmos. Chem. Phys. 8, 1329–1341.

Nakajima, T., Yoon, S.C., Ramanathan, V., Shi, G.Y., Takemura, T., Higurashi, A., Takamura, T., Aoki, K., Sohn, B.J., Kim, S.W., Tsuruta, H., Sugimoto, N., Shimizu, A., Tanimoto, H., Sawa, Y., Lin, N.H., Lee, C.T., Goto, D., Schutgens, N., 2007. Overview of the Atmospheric Brown Cloud East Asian Regional Experiment 2005 and a study of the aerosol direct radiative forcing in East Asia. J. Geophys. Res.-Atmos. 112.

Nam, J., Wang, Y., Luo, C., Chu, D.A., 2010. Trans-Pacific transport of Asian dust and CO: accumulation of biomass burning CO in the subtropics and dipole structure of transport. Atmos. Chem. Phys. 10, 3297–3308.

Ohara, T., Akimoto, H., Kurokawa, J., Horii, N., Yamaji, K., Yan, X., Hayasaka, T., 2007. An Asian emission inventory of anthropogenic emission sources for the period 1980–2020. Atmos. Chem. Phys. 7, 4419–4444.

Onishi, K., Kurosaki, Y., Otani, S., Yoshida, A., Sugnimoto, N., Kurozawa, Y., 2012. Atmospheric transport route determines components of Asian dust and heal effects in Japan. Atmos. Environ. 49, 94–102.

Pham, T.B.T., Manomaiphiboon, K., Vongmahadlek, C., 2007. Updated emission estimates of ozone precursors from energy consumption by power plants and industrial facilities in the central and eastern regions of Thailand. Asian J. Energy Environ. 08 (01), 483e489.

Reid, J.S., Hyer, E.J., Prins, E.M., Westphal, D.L., Zhang, J.L., Wang, J., Christopher, S.A., Curtis, C.A., Schmidt, C.C., Eleuterio, D.P., Richardson, K.A., Hoffman, J.P., 2009. Global monitoring and forecasting of biomass-burning smoke: description of and lessons from the fire locating and modeling of burning emissions (FLAMBE) program. IEEE J. Sel. Top. Appl. Earth Obs. Remote Sens. 2, 144–162.

Reid, J.S., Hyer, E.J., Johnson, R.S., Holben, B.N., Yokelson, R.J., Zhang, J.L., Campbell, J.R., Christopher, S.A., Di Girolamo, L., Giglio, L., Holz, R.E., Kearney, C., Miettinen, J., Reid, E.A., Turk, F.J., Wang, J., Xian, P., Zhao, G.Y., Balasubramanian, R., Chew, B.N., Janjai, S., Lagrosas, N., Lestari, P., Lin, N.H., Mahmud, M., Nguyen, A.X., Norris, B., Oanh, N.T.K., Oo, M., Salinas, S.V., Welton, E.J., Liew, S.C., 2013. Observing and understanding the Southeast Asian aerosol system by remote sensing: an initial review and analysis for the Seven Southeast Asian Studies (7SEAS) program. Atmos. Res. 122, 403–468.

Sayer, A.M., Hsu, N.C., Bettenhausen, C., Jeong, M.-J., Holben, B.N., Zhang, J., 2012. Global and regional evaluation of over-land spectral aerosol optical depth retrievalsfrom SeaWiFS. Atmos. Meas. Tech. 5, 1761–1778.

Shimizu, A., Sugimoto, N., Matsui, I., Nishizawa, T., 2014. Direct comparison of extinction coefficients derived from Mie-scattering lidar and number concentrations of particles, subjective weather report in Japan. J. Quant. Spectrosc. Radiat. Transf. 153, 77–87.

Skamarock, W.C., Klemp, J.B., Dudhia, J., Gill, D.O., Barker, D.M., Duda, M.G., Huang, X.Y., Wang, W., Powers, J.G., 2008. A Description of the Advanced Research WRF Version 3. NCAR.

Streets, D.G., Yarber, K.F., Woo, J.H., Carmichael, G.R., 2003. Biomass burning in Asia: annual and seasonal estimates and atmospheric emissions. Glob. Biogeochem. Cycles 17. http://dx.doi.org/10.1029/2003GB002040.

Tang, Y.H., Carmichael, G.R., Uno, I., Woo, J.H., Kurata, G., Lefer, B., Shetter, R.E., Huang, H., Anderson, B.E., Avery, M.A., Clarke, A.D., Blake, D.R., 2003a. Impacts of aerosols and clouds on photolysis frequencies and photochemistry during TRACE-P: 2. Three-dimensional study using a regional chemical transport model. J. Geophys. Res.-Atmos. 108.

Tang, Y.H., Carmichael, G.R., Woo, J.H., Thongboonchoo, N., Kurata, G., Uno, I., Streets, D.G., Blake, D.R., Weber, R.J., Talbot, R.W., Kondo, Y., Singh, H.B., Wang, T., 2003b. Influences of biomass burning during the Transport and Chemical Evolution Over the Pacific (TRACE-P) experiment identified by the regional chemical transport model. J. Geophys. Res.-Atmos. 108.

Thao, P.T.B., Junpen, A., Cheewapongpham, P., Boonman, T., Garivait, S., Chatani, S., Kojima, K., 2014. Bottom-up inventory of air pollutants emissions from power generation in Thailand. In: 16th GEIA Conference, Colorado, USA.

The State Council of the People's Republic of China, 2011. The Twelfth Five-Year Plan for Environmental Protection (available at www.gov.cn/zwgk/2011-12/20/content 2024895.htm) (in Chinese).

Tsay, S.C., Hsu, N.C., Lau, W.K.M., Li, C., Gabriel, P.M., Ji, Q., Holben, B.N., Welton, E.J., Nguyen, A.X., Janjai, S., Lin, N.H., Reid, J.S., Boonjawat, J., Howell, S.G., Huebert, B.J., Fu, J.S., Hansell, R.A., Sayer, A.M., Gautam, R., Wang, S.H., Goodloe, C.S., Miko, L.R., Shu, P.K., Loftus, A.M., Huang, J., Kim, J.Y., Jeong, M.J., Pantina, P., 2013. From BASE-ASIA toward 7-SEAS: a satellite-surface perspective of boreal spring biomass-burning aerosols and clouds in Southeast Asia.

Atmos. Environ. 78, 20–34.
Ummer, K., 2012. CARMA Revisited: an Updated Database of Carbon Dioxide Emissions from Power Plants Worldwide. Working Paper Number 304. Center for Global Development.
van der Werf, G.R., Dempewolf, J., Trigg, S.N., Randerson, J.T., Kasibhatla, P.S., Gigliof, L., Murdiyarso, D., Peters, W., Morton, D.C., Collatz, G.J., Dolman, A.J., DeFries, R.S., 2008. Climate regulation of fire emissions and deforestation in equatorial Asia. Proc. Natl. Acad. Sci. U. S. A. 105, 20350–20355.
van der Werf, G.R., Randerson, J.T., Giglio, L., Collatz, G.J., Mu, M., Kasibhatla, P.S., Morton, D.C., DeFries, R.S., Jin, Y., van Leeuwen, T.T., 2010. Global fire emissions and the contribution of deforestation, savanna, forest, agricultural, and peat fires (1997–2009). Atmos. Chem. Phys. 10, 11707–11735.
Wang, S.H., Lin, N.H., Chou, M.D., Woo, J.H., 2007. Estimate of radiative forcing of Asian biomass-burning aerosols during the period of TRACE-P. J. Geophys. Res.-Atmos. 112.
Wang, S.X., Zhao, M., Xing, J., Wu, Y., Zhou, Y., Lei, Y., He, K.B., Fu, L.X., Hao, J.M., 2010. Quantifying the air pollutants emission reduction during the 2008 Olympic Games in Beijing. Environ. Sci. Technol. 44, 2490–2496.
Wang, S.X., Xing, J., Chatani, S., Hao, J.M., Klimont, Z., Cofala, J., Amann, M., 2011. Verification of anthropogenic emissions of China by satellite and ground observations. Atmos. Environ. 45, 6347–6358.
Watanabe, M., Kurai, J., Shimizu, E., 2014. Influence of Asian dust storm on Asthma in Western Japan. Genes Environ. 36, 137–144.
Wheeler, D., Ummer, K., 2008. Calculating CARMA: Global Estimation of CO2 Emission from the Power Sector. Working Paper Number 145. Center for Global Development.
World Health Organization, 2011. Burden of Disease Attributable to Outdoor Air Pollution. Geneva.
World Health Organization, 2014. Burden of Disease Attributable to Outdoor Air Pollution. Geneva.
Yang, Y.Q., Wang, J.Z., Niu, Ta, Zhou, C.H., Chen, M., Liu, J.Y., 2013. The variability of spring sand-dust frequency in Northeast Aisa from 1980 to 2011. J. Meteorol. Res. 27 (1), 119–127.
Zhang, Q., Streets, D.G., Carmichael, G.R., He, K.B., Huo, H., Kannari, A., Klimont, Z., Park, I.S., Reddy, S., Fu, J.S., Chen, D., Duan, L., Lei, Y., Wang, L.T., Yao, Z.L., 2009. Asian emissions in 2006 for the NASA INTEX-B mission. Atmos. Chem. Phys. 9, 5131–5153.
Zhang, R., Bian, Q., Fung, J.C.H., Lau, A.K.H., 2013. Mathematical modeling of seasonal variations in visibility in Hong Kong and the Pearl River Delta region. Atmos. Environ. 77, 803–816.
Zhao, B., Wang, S.X., Dong, X.Y., Wang, J.D., Duan, L., Fu, X., Hao, J.M., Fu, J., 2013a. Environmental effects of the recent emission changes in China: implications for particulate matter pollution and soil acidification. Environ. Res. Lett. 8.
Zhao, B., Wang, S.X., Wang, J.D., Fu, J.S., Liu, T.H., Xu, J.Y., Fu, X., Hao, J.M., 2013b. Impact of national NOx and SO2 control policies on particulate matter pollution in China. Atmos. Environ. 77, 453–463.